VELOCITY STATISTICS AND STRUCTURE IN PIPE TURBULENCE DERIVED FROM A SIMPLE CRITICAL-LAYER MODEL

A S Sharma

Department of Aeronautics
Imperial College
London, SW7 2AZ UK
ati@imperial.ac.uk

B J McKeon

California Institute of Technology,
Pasadena,
CA 91125, U.S.A.
mckeon@caltech.edu

ABSTRACT

We describe the development of a simple forcing-response analysis of the Navier-Stokes equations that predicts important structural and scaling features of wall turbulence. In particular, we propose an economical explanation for the meandering appearance of very large scale motions observed in turbulent pipe flow, and likewise demonstrate that hairpin vortices are predicted, using a simple linear superposition of modes derived from the model. The computationally cheap approach explains and predicts vortical structures and velocity statistics of turbulent flows that have previously been identified only in experiments or by direct numerical simulation. This new capability has clear implications for modeling, simulation and control of a ubiquitous class of wall flows.

INTRODUCTION

In flows of the most widely-ranging practical interest, namely flows over surfaces or *wall turbulence*, the turbulence problem is greatly complicated by inhomogeneity in the wall-normal direction caused by the no-slip and no-penetration boundary conditions at the wall.

Turbulent fluctuations of velocity and pressure have characteristics of chaotic motion, and a common feature of wall turbulence is the presence of persistent, coherent vortical structures which inhabit distinct regions of the flow (Theodorsen, 1952; Schoppa & Hussain, 2002) and have been generally believed to be dominated by nonlinear dynamics. These observations of distinct classes of coherent structure in parallel with the measurement of turbulent velocity statistics over the last sixty or more years have led to a dichotomy in the understanding of the formation, development and scaling of even the simplest, canonical turbulent wall flows, such as flow through straight channels and pipes, or flow over a flat plate in the absence of a pressure gradient.

In this paper, we demonstrate that the formation of such coherent structures is a natural consequence of the velocity field that arises as a near-singular response of the linearised equations of motion to the wave-like forcing arising due to nonlinear interactions with other wave-like motions. The framework provides predictive information both about how the wall-normal distribution of turbulent energy of the velocity field shows self-similarity across Reynolds numbers, and also describes the wall-normal coherence of structures within the flow. The predictions of the scaling and distribution of second-order velocity statistics, and of structural characteristics are provided using an essentially linear model. The analysis uses only the Navier-Stokes equations and an assumed mean velocity profile.

There have been many observations of a common structural pattern described as a hairpin vortex (a vortical loop with legs originating close to the wall, a body inclined in the downstream direction and a sense of rotation consistent with the vorticity associated with the mean shear) in both experiment and simulation (Head & Bandyopadhyay, 1981; Adrian *et al.*, 2000; Adrian, 2007; Wu & Moin, 2008), while the attached eddy hypothesis formulated by Townsend (1956) and Perry & Chong (1982) in the mid-20th century has sought to use phenomenological arguments to determine the velocity field associated with hierarchies of these structures. Nonlinear mechanisms for the formation and growth of packets of hairpins in otherwise quiescent flow have also been proposed by Zhou *et al.* (1996), while there remains controversy as to whether they are simply a remnant of the transition to turbulence, or even whether whole hairpins, rather than a statistical vortical imprint, even exist.

With alternative models lacking, statistical descriptions have remained the simplest method to obtain comprehensive descriptions of the turbulent field. Under the assumptions of stationarity and ergodicity, simple spectral representations provide information on important scales in the flow. While information at streamwise and spanwise wavenumber and tem-

poral frequency (k, n, ω, respectively) is required to fully describe the flow, usually one-dimensional (integrated) spectra are reported due to the intensive nature of obtaining and storing information in three dimensions. The streamwise spectra reveal the presence of the widest range of scales, from the Kolmogorov scales (Kolmogorov, 1941, 1962) responsible for small-scale dissipation of energy up to so-called *very large scale motions (VLSMs)* of the order of ten times the length scale imposed by the flow geometry (typically the pipe radius, or the boundary layer thickness). Monty *et al.* (2007) inferred that the VLSMs reach lengths of the order of thirty radii when spanwise *meander* of the coherent region is taken into account.

A recent focus of research has been on the origin and development of large and small scales, and how their competing influences lead to trends with increasing Reynolds number. While the origin of the VLSMs has remained elusive, there has been recent progress in predicting velocity statistics by considering the nature of their spectral interaction with the energetic near-wall region (Mathis *et al.*, 2009; Marusic *et al.*, 2010). A truly complete interpretation of a turbulent flow field requires assimilation of both the velocity statistics and vortical structures; observational progress has been made by considering the generation of one by the other, posing a classic "chicken and egg" conundrum. In the absence of low-order or simple predictive models for turbulent flows, the only current recourse for the fluid mechanician who wishes to quantify the state of turbulence lies in expensive simulations or experiments.

In the following we examine the response of the linearised flow to harmonic forcing. In this picture, the observed behaviour is explained by even small forcing on the system leading to energetic flowfield response (Bamieh & Dahleh, 2001; Jovanovic & Bamieh, 2005). The idea of linear processes as important in turbulent flow dates back at least to Malkus (1956). The device of identifying the nonlinear interaction between Fourier modes in the Navier-Stokes equations (NSE) as a forcing actually acting on the a linear system permits the extension of such methods to fully developed turbulent flows (McKeon & Sharma, 2010), allowing the successful prediction of observed features of turbulent flow.

A FORCING-RESPONSE MODEL

We consider turbulent flow through a long straight pipe with a cylindrical cross-section. Laminar flow in this geometry is stable to infinitesimal disturbances, and the transition to turbulence is still not completely understood (Hof *et al.*, 2010), but the pipe offers the analytical benefits of statistical homogeneity in the streamwise direction and a simple constraint on the azimuthal wavenumber. Turbulent flow through pipes is important for applications like the transport of fluids such as oil and natural gas, and also in numerous natural and biomedical applications, and is also highly relevant to the study of other canonical flows.

We defined Reynolds number as the ratio between the pipe radius R and the viscous length scale defined by v/u_τ, where v is the kinematic viscosity of the fluid and u_τ is a velocity scale associated with the skin friction acting on the wall, τ, and the fluid density, thus $R^+ = Ru_\tau/v$.

McKeon & Sharma (2010) recently formulated a travel-ing wave framework by which to analyze the dominant velocity mode shapes at particular wavenumber-frequency combinations. The fully turbulent velocity vecotr field, **v**, can be represented in a divergence-free basis as a superposition of Fourier modes at various spatial wavenumbers and temporal frequencies with wall-normal variation (waves),

$$\mathbf{v}(y,x,\theta,t) = \sum_n \int_{-\infty}^{\infty} \int_{-\infty}^{\infty} \mathbf{v}_{kn\omega}(y)e^{i(\omega t - kx - n\theta)}dk\,d\omega \quad (1)$$

where y is the wall-normal distance, k and n are the wavenumbers in the streamwise (x) and azimuthal (θ) directions, all normalized with the pipe radius, and ω is the temporal frequency with respect to time t.

These helical waves represent the transmission of fluctuating energy relative to the mean flow. We treat the steady component (the mean flow) separately,

$$\tilde{\mathbf{v}} = \mathbf{v} - \mathbf{v}_{000} \quad (2)$$

Under this decomposition, the Navier-Stokes equations can be written in an input-output formulation, where the characteristics of the linear operator $\mathscr{L}_{kn\omega}(y)$ describe the velocity field's response to an unmodelled harmonic forcing **f**, itself arising from the nonlinear interactions between the velocity field at other wavenumber-frequency combinations,

$$\mathbf{f}_{kn\omega} = (\tilde{\mathbf{v}} \cdot \nabla \tilde{\mathbf{v}})_{kn\omega} \quad (3)$$

The equations expressed in this form are

$$\mathbf{v}_{kn\omega}(y) = (i\omega - \mathscr{L}_{kn\omega}(y))^{-1}\mathbf{f}_{kn\omega}(y) \quad (4)$$

and the operator $(i\omega - \mathscr{L}_{kn\omega}(y))^{-1}$ relating the forcing to the velocity field response is called the *resolvent*.

The analysis up to this point is very similar to the development of the linearized, fourth-order Orr-Sommerfeld-Squire operator of linear stability theory, with the exceptions that the $(k,n,\omega) = (0,0,0)$ mode is identified as the turbulent mean velocity rather than the laminar solution, and the nonlinear forcing terms are explicitly retained in the present analysis. As such, concepts relevant to the study of neutrally-stable disturbances in inviscid, linearized laminar flow can be extended to the turbulent case, with the understanding that in the latter case the waves are lightly damped and would asymptotically decay in the absence of forcing **f**.

The resolvent has a nearly-singular, essentially inviscid response at the *critical layer*, where the local mean velocity U is equal to the streamwise convective velocity of the wave.

Given the very selective response of the flow, we may hypothesise that the velocity field is dominated by the largest possible response to forcing, at any given wavenumber and frequency set. Mathematically, we may find and order these orthogonal *response modes* by a *Schmidt decomposition* (Young, 1988) of the resolvent into two sets of unitary orthogonal basis functions, which provides, for a given forcing magnitude, the largest possible velocity field response, the second

largest and so on.[1] In practice, we find that the velocity field given by the first of these response modes is associated with a response typically one to many orders of magnitude larger than that of the second mode. The velocity field observed in a real flow will therefore be well described by the first response mode if the forcing contains a non-negligible component of the correct shape. This assumption of selective response is congruent with an assumption that the resolvent may be approximated by a low rank operator (which has been postulated in various forms by many previous researchers). The Schmidt decomposition of the resolvent is

$$(i\omega I - \mathscr{L}_{kn\omega}(y))^{-1} = \sum_{j=1}^{\infty} \psi_{jkn\omega}(y)\sigma_{jkn\omega}\phi_{jkn\omega}(y) \quad (5)$$

with

$$\int_y \phi_{lkn\omega}(y)\phi_{mkn\omega}(y)dy = \delta_{lm}$$

$$\int_y \psi_{lkn\omega}(y)\psi_{mkn\omega}(y)dy = \delta_{lm}$$

$$\sigma_j \geq \sigma_{j+1} \geq 0$$

Under the further assumption of forcing that is small relative to the magnitude of the response modes, a standard asymptotic analysis (Drazin & Reid, 2004) can be used to describe the scaling of the two regions where viscous effects are required: firstly at the critical layer (to regularize the singularity of the inviscid problem) and at the wall (to meet the wall boundary condition). We call a response mode in which viscous modification at the wall dominates, a *wall* or *attached* mode, and we call a response mode where viscous modification at the critical layer dominates a *critical* mode.

STATISTICAL PREDICTIONS

In contrast to calculating statistics at a single wall-normal location (y) at a given Fourier wavenumber, the response modes provide a basis that predicts the wall-normal amplitude and phase variation of the velocity field. To date, we have examined the structure of the response modes up to a Reynolds number of $R^+ = 2 \times 10^4$, of the same order of magnitude as conditions in, for example, a transcontinental natural gas pipeline (McKeon, 2010). Here we present key results at $R^+ = 2 \times 10^3$, a condition that is achievable in both experiment and state-of-the-art simulation.

Figure 1 shows the streamwise velocity component arising from a combination of the left and right going helical velocity response modes with a wavenumber-frequency combination representative of the dominant motion near the wall, namely streamwise and spanwise wavelengths of a thousand and one hundred viscous units, respectively, and a convection velocity of ten times the friction velocity, $(\lambda_x^+, \lambda_z^+, U_x^+) = (1000, 100, 10)$. The distinctive pattern of rolling motions

---

[1]The calculations are performed using a modified version of the approach of Meseguer & Trefethen (2003) and the experimental mean velocity data of McKeon *et al.* (2004).
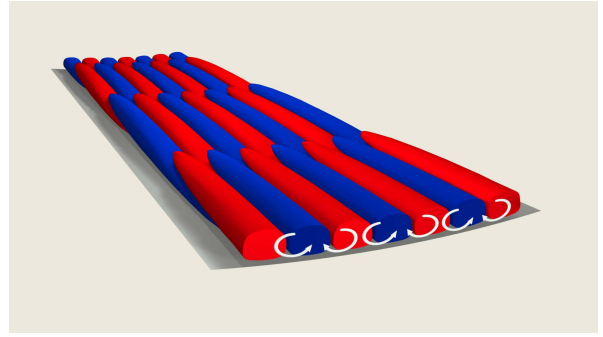

Figure 1. Shape of the first singular mode representative of the dominant near wall motions, $(\lambda_x^+, \lambda_z^+, U_x^+) = (1000, 100, 10)$. Color denotes isosurfaces of streamwise velocity (streaks), where red and blue correspond to high and low velocity respectively relative to the mean flow (heading into the page), and the arrows show the sense of the in-plane velocity field.
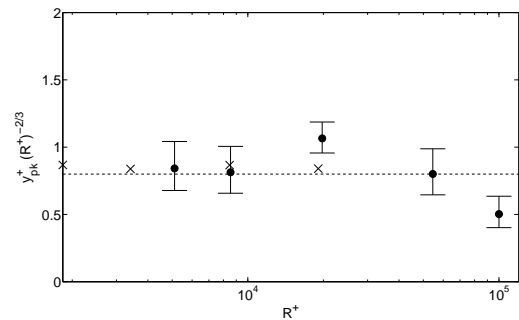

Figure 2. Variation of VLSM energy peak with Reynolds number: ($\times$) model prediction at $(k, n, \omega) = (1, 10, \frac{2}{3}U_{CL})$, (- -) theoretical prediction of $y^+ = 0.8(R^+)^{2/3}$, ($\bullet$) Superpipe data (McKeon, 2008). Note that probe resolution may impact the experimental result at the highest Reynolds number.

aligned in the streamwise direction and strong, alternating inclined streaks of fast and slow streamwise velocity u shown in Figure 1 is entirely consistent with visual and quantitative observations of the near-wall region in canonical flows (Schoppa & Hussain, 2002). In McKeon & Sharma (2010), we showed that the wall-normal location of the peak intensity of u associated with this mode is independent of Reynolds number. This scaling result is borne out by experimental measurements over a range of Reynolds numbers.

Our framework can also be used predictively to describe the Reynolds number dependence of the location of peak VLSM energy, y_{pk}^+, and to understand the origin of VLSMs. A mode that is both attached to the wall and critical has a special significance. In pipe flow, for parameters representative of a VLSM, $(k, n) = (1, 10)$ approximately, this condition occurs when the convective velocity is two-thirds of the centerline velocity, independent of Reynolds number, leading to the prediction

$$y_{pk}^+ = 0.8(R^+)^{2/3} \quad (6)$$

3

The agreement between this theoretically derived expression and the experimental results of Morrison *et al.* (2004) reported by McKeon (2008) is remarkably good, as shown in Figure 2 from McKeon & Sharma (2010). This prediction differs from the $(R^+)^{1/2}$ law appropriate for a boundary layer.

STRUCTURAL PREDICTIONS

Having described important statistical aspects of pipe flow, we now turn our attention to structural considerations. A simple superposition of first response modes at different wavenumber-frequency combinations also sheds light on the controversy surrounding the true length of the VLSM motions. Even the addition of the velocity fields corresponding to only two additional pairs of response modes with similar amplitudes to the VLSM mode described above quickly leads to the observation of apparently meandering structures with length far greater than six radii, as shown in Figure 3. The visual similarity is striking to experimental data shown in the lowest panel of the figure (from Monty *et al.* (2007)). The meandering phenomenon is an artefact of the many response modes that are present in a real flow combining with the energetic content of the VLSM itself, effectively decorrelating the VLSM mode.

The three-dimensional velocity field associated with the attached near-wall mode shown in Figure 1 gives an intuitive hint as to the locations of coherent vorticity associated with this type of mode. We identify structure through measures which distinguish between the shear and rotational components of vorticity, namely the symmetric and anti-symmetric components of the velocity gradient tensor, $\nabla \mathbf{v}$. While any of the commonly used measures (Chakraborty *et al.*, 2005) give very similar results, we highlight isosurfaces of *swirling strength*[2] for a wall mode with $(k, n, \omega) = (4.5, \pm 10, 1.67)$ in Figure 4 (upper panel). The surfaces are colored by the magnitude of the azimuthal vorticity, with blue corresponding to *prograde* vortices, with the same sense of rotation as the traditional hairpin, and red to *retrograde* vortices, with the opposite sense of rotation. The latter have been reported in the literature to occur relatively infrequently (Natrajan *et al.*, 2007; Carlier & Stanislas, 2005). Our model predicts an equal distribution of prograde and retrograde vortices associated with each wall mode. However, in the presence of a mean velocity profile with decreasing shear in the wall-normal direction, the retrograde vortices are suppressed while the prograde ones are reinforced, leading to a distribution of vortices that is consistent with experimental observations, Figure 4 (lower panel). In this figure, the mean shear is sufficiently strong to completely suppress the retrograde vortices below the swirl threshold selected for plotting. We emphasize that the swirl field regenerated from the full range of modes projected out, for example, from a direct numerical simulation would reproduce the full swirl field: we explore here a decomposition of the swirl field around the mean shear, which precludes consideration of the contribution of hairpin heads to the mean shear itself, as explored by other authors such as Adrian *et al.* (2000). There are two points to note here, firstly, this is a simple manifestation of the mean shear

---

[2]λ_{ci}, or the imaginary part of the complex conjugate eigenvalue pair associated with the velocity gradient tensor
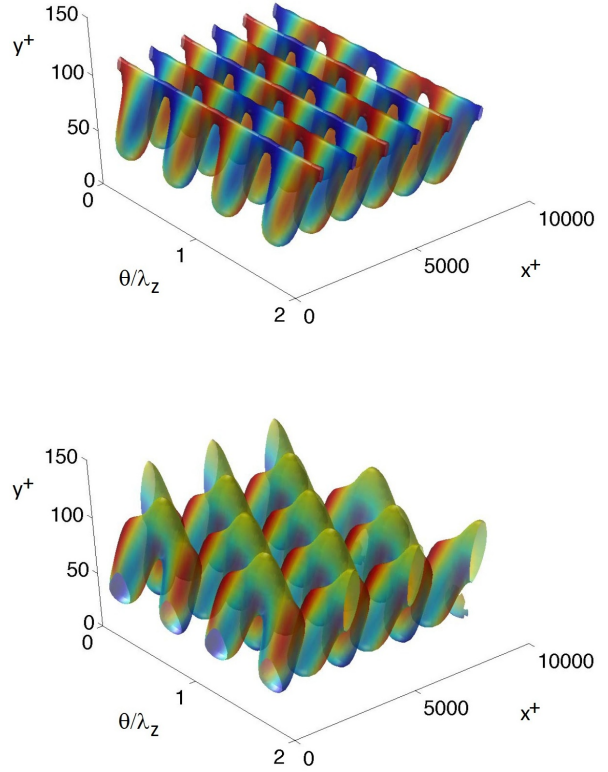

Figure 4. Isosurfaces of constant swirling strength for the $(k, n, \omega) = (4.5, \pm 10, 1.67)$ velocity response mode (three wavelengths are shown in the streamwise and two in the spanwise directions) at $R^+ = 1800$, color-coded with the sense of the azimuthal rotation. Blue and red denote pro- and retrograde swirl (or rotation in and counter to the sense of the classical hairpin vortex), respectively. *Upper panel:* under a Galilean transformation (i.e. constant convection velocity subtracted throughout the field of view) there are even numbers of prograde and retrograde vortices. *Lower panel:* with the mean velocity profile added, the retrograde vortices disappear and the prograde ones are strengthened.

being the only net source of azimuthal vorticity, and secondly, swirling strength is not a distributive operation. In other words, swirl($a+b$) $\neq$ swirl(a) + swirl(b). Thus the phenomenon is a direct consequence of the diagnostics commonly used to identify structure.

It is clear that a very complex velocity field can be obtained simply by superposing modes with different (k, n, ω) (and therefore different convective velocities) and amplitudes, and with associated local velocity gradients. Critically, because swirling strength is not distributive, the swirl field cannot be simply determined from a superposition of the swirling strength associated with the individual response modes.

Aspects of the vortical structure and velocity statistics associated with turbulent flows are typically explained only in phenomenological terms and have been identified only in
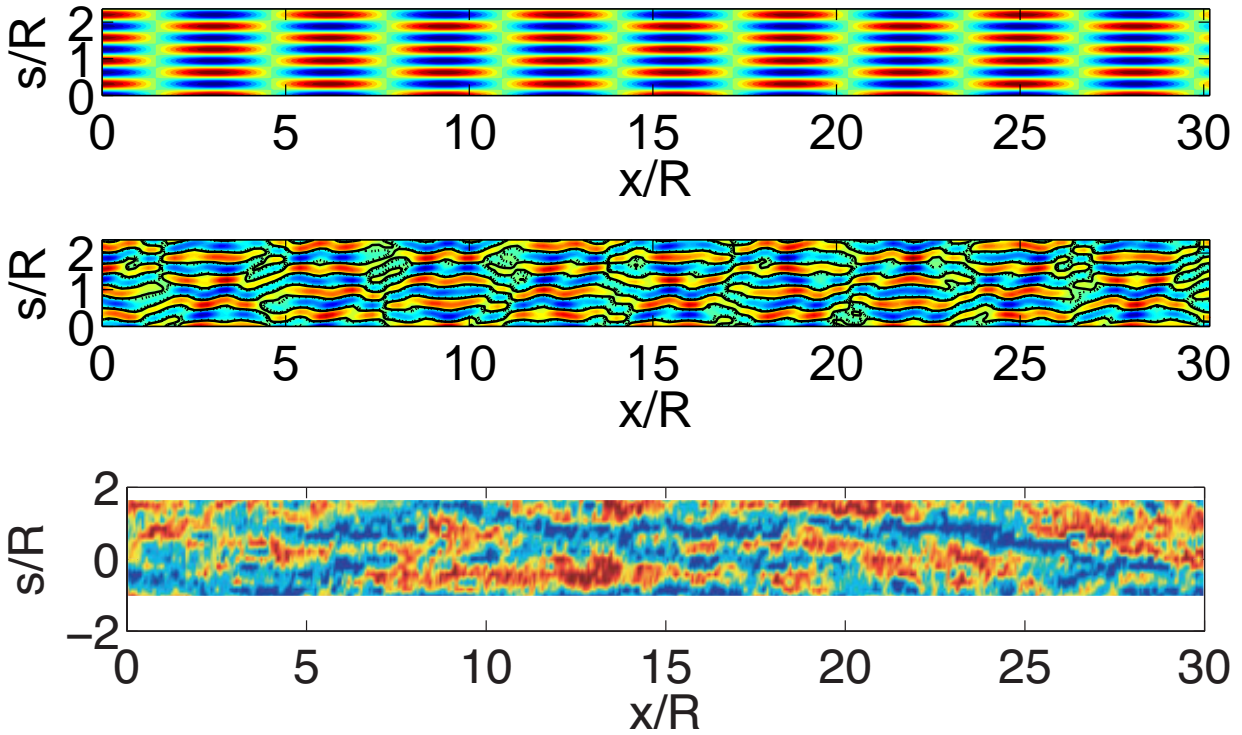
Figure 3. An explanation of apparent "meandering" of the VLSMs. The top panel contains isosurfaces of the streamwise velocity at $y/R = 0.15$ for the summation of left- and right-going VLSM modes and the middle panel shows how even longer coherence, of the order of the panel length, can be obtained by superposing the velocity response mode pair fields from two additional (shorter) modes with $(k, n, \omega) = (4.7, \pm 12, 0.2)$ and $(6.2, \pm 15, 0.6)$ with amplitude 75% of the VLSM modes. The bottom panel shows the experimental results of Monty *et al.* (2007).

experiments or computationally costly direct numerical simulation. The linearity of the processes driving wall turbulence permits superposition of the response modes. This linearity is revealed by formulating the NSE as a forcing-response problem. We have studied pipe flow in the current work, but the same approach can be applied to both internal and external flows with simple modifications. The results shown in this paper were generated in seconds using a standard laptop computer, and the approach extends to higher Reynolds numbers. The only limitation is the numerical precision required to deal with the near-singular response to the most amplified forcing.

The results offer some reconciliation of the statistical and structural interpretations of such flows by working from the NSE and an assumed mean profile. The understanding of the different types of mode and where they occur in the flow has significant implications for the prediction of Reynolds number trends and the modeling of turbulent activity at reduced computational cost. While the forcing is currently unstructured, such that we do not determine the appropriate amplitudes at individual modes, the possibility to "close the loop" and formulate a reduced order model of turbulent pipe flow is compelling: under a self-consistent combination of modes the assumed mean velocity profile will be generated, such that a self-sustaining system can be designed. The potential to design rigorous control techniques for such a system with the objective of enforcing favorable turbulence characteristics is a natural, and plausible, next step.

REFERENCES

Adrian, R. J. 2007 Vortex organization in wall turbulence. *Phys. Fluids* **19** (041301).

Adrian, R. J., Meinhart, C. D. & Tomkins, C. D. 2000 Vortex organization in the outer region of the turbulent boundary layer. *J. Fluid Mech.* **422**, 1–54.

Bamieh, B. & Dahleh, M. 2001 Energy amplification in channel flows with stochastic excitation. *Phys. Fluids* **13** (11), 3258–3269.

Carlier, Johan & Stanislas, Michel 2005 Experimental study of eddy structures in a turbulent boundary layer using particle image velocimetry. *Journal of Fluid Mechanics* **535**, 143–188.

Chakraborty, P., Balachandar, S. & Adrian, R. J. 2005 On the relationships between local vortex identification schemes. *J. Fluid Mech.* **535**, 189–214.

Drazin, P. G. & Reid, W. H. 2004 *Hydrodynamic Stability*, 2nd edn. Cambridge University Press.

Head, M. R. & Bandyopadhyay, P. R. 1981 New aspects

of turbulent boundary-layer structure. *J. Fluid Mech.* **107**, 297–337.

Hof, B., de Lozar, A., Avila, M., Tu, X. & Schneider, T. M. 2010 Eliminating turbulence in spatially intermittent flows. *Science* **327**, 1491–1494.

Jovanovic, M. R. & Bamieh, B. 2005 Componentwise energy amplification in channel flows. *J. Fluid Mech.* **534**, 145–183.

Kolmogorov, A. N. 1941 The local structure of turbulence in incompressible viscous fluid for very large Reynolds numbers. *Dokl. Akad. Nauk. SSSR* **30** (4).

Kolmogorov, A. N. 1962 A refinement of previous hypotheses concerning the local structure of turbulence in a viscous compressible fluid at high Reynolds numbers. *J. Fluid Mech.* **13**, 82–85.

Malkus, W. V. R. 1956 Outline of a theory of turbulent shear flow. *Journal of Fluid Mechanics* **1** (05), 521–539.

Marusic, I., Mathis, R. & Hutchins, N. 2010 Predictive model for wall-bounded turbulent flow. *Science* **329** (5988), 193–196.

Mathis, R., Hutchins, N. & Marusic, I. 2009 Large-scale amplitude modulation of the small-scale structures of turbulent boundary layers. *J. Fluid Mech.* **628**, 311–337.

McKeon, B. J. 2008 Scaling in wall turbulence: scale separation and interaction. *AIAA Paper* **2008-4237**.

McKeon, B. J. 2010 Controlling turbulence. *Science* **327**, 1462–1463.

McKeon, B. J., Li, J., Jiang, W., Morrison, J. F. & Smits, A. J. 2004 Further observations on the mean velocity distribution in fully developed pipe flow. *J. Fluid Mech.* **501**, 135–147.

McKeon, B. J. & Sharma, A. S. 2010 A critical layer model for turbulent pipe flow. *J. Fluid Mech.* **658**, 336–382.

Meseguer, A. & Trefethen, L. N. 2003 Linearized pipe flow to Reynolds number 10^7. *J. Comp. Phys.* **186**, 178–197.

Monty, J. P., Stewart, J. A., Williams, R. C. & Chong, M. S. 2007 Large-scale features in turbulent pipe and channel flows. *J. Fluid Mech.* **589**, 147–156.

Morrison, J. F., Jiang, W., McKeon, B. J. & Smits, A. J. 2004 Scaling of the streamwise velocity component in turbulent pipe flow. *J. Fluid Mech.* **508**, 99–131.

Natrajan, V. K., Wu, Y. & Christensen, K. T. 2007 Spatial signatures of retrograde spanwise vortices in wall turbulence. *J. Fluid Mech.* **574**, 155–167.

Perry, A. E. & Chong, M. S. 1982 On the mechanism of wall turbulence. *J. Fluid Mech* **119**, 173–217.

Schoppa, W. & Hussain, F. 2002 Coherent structure generation in near-wall turbulence. *J. Fluid Mech.* **453**, 57–108.

Theodorsen, T. 1952 Mechanism of turbulence. In *Proc. 2nd Midwestern Conf. on Fluid Mech.*, pp. 1–19. Ohio State University, Columbus, Ohio.

Townsend, A. A. 1956 *The Structure of Turbulent Shear Flow*. Cambridge University Press.

Wu, X. & Moin, P. 2008 A direct numerical simulation study on the mean velocity characteristics in pipe flow. *J. Fluid Mech.* **608**, 81–112.

Young, N. 1988 *An Introduction to Hilbert Space*. Cambridge, UK: Cambridge University Press.

Zhou, J., Adrian, R. J. & Balachandar, S. 1996 Autogeneration of near wall vortical structure in channel flow. *Phys. Fluids* **8**, 288–291.